The Versatile Roles of Graphene in Organic Photovoltaic Device Technology

Jayalekshmi Sankaran and Sreekanth J. Varma

> The pursuit of truth continues; it is enticing, when each giant leap brings in, new surprises.

Abstract This chapter discusses the potential applications of graphene in the realization of efficient and stable organic optoelectronic devices, especially flexible solar cells. With the introduction of the prospects of graphene and functionalized graphene in modifying the performance characteristics of organic solar cells, the chapter evolves into assessing the prospects of realizing all carbon photovoltaic devices. The combination of unique, yet tunable, electrical and optical properties of graphene, makes it a highly sought after candidate for various technologically important applications in optoelectronics. Graphene has been identified as a suitable replacement for the highly expensive, brittle and less abundant indium tin oxide, as the transparent electrode material for optoelectronic device applications. The best graphene-based transparent conducting films show very low sheet resistance of 20 Ω/sq and high transparency around 90 % in the visible spectrum, making it a better choice compared to the commonly used transparent conductors including indium tin oxide (ITO) and zinc oxide (ZnO). The absence of energy band gap in graphene has originally limited its applications in optoelectronic devices. This problem has since been solved with the advent of graphene nanoribbons (GNRs) and functionalized graphenes. Functionalized graphenes and GNRs have extended the use of graphene as hole and electron transport layers in organic/polymer light emitting diodes and organic solar cells by the suitable tuning of the band gap energy. Blending dispersions of functionalised graphene with the active layers in photovoltaic devices has been found to enhance light absorption and enable carrier transport efficiently. Graphene layers with absorption in the entire visible region can be fine-tuned to be incorporated into the active layers of organic solar cells. Finally

J. Sankaran (✉)
Department of Physics, Cochin University of Science and Technology, 682022 Cochin, Kerala, India
e-mail: lakshminathcusat@gmail.com; jayalekshmi@cusat.ac.in

S.J. Varma
Department of Physics, Sanatana Dharma College, 688003 Alapuzha, Kerala, India
e-mail: sreekanthvarma@gmail.com

P. Misra (ed.), *Applied Spectroscopy and the Science of Nanomaterials*,
Progress in Optical Science and Photonics 2, DOI 10.1007/978-981-287-242-5_10

the synthesis conditions of GNRs and the functionalized graphenes can be optimized to achieve the required structural, optical and electrical characteristics for venturing into developing all carbon-based cost-effective organic solar cells with improved efficiency.

Keywords Graphene · Graphene nanoribbons (GNRs) · Functionalized graphene · Organic solar cells · Photovoltaics · Indium tin oxide · Zinc oxide · Polymer light emitting diodes (LEDs) · Organic LEDs · Electronic devices · All carbon photovoltaic devices

1 Introduction

The past few decades have witnessed unparalleled technological innovations capable of influencing all walks of human activity and enrich the intellectual pursuits in the realization of a sustainable and green living ambience with the added flavors of hitherto unimaginable comfort and luxury. In this context, the possibilities of Nanoscience and Technology have revolutionized the conventional perspectives in the design strategies of the major categories of devices that empower the energy requirements of the present day society. Of the various categories of nanostructures developed and investigated, carbon-based nanostructures have gained an upper hand, by virtue of their intriguing and often exciting characteristics with visionary prospects as the building blocks of new surprises yet to be unveiled. The three important carbon-based nanostructures, the graphene, the carbon nanotubes and the fullerenes, all stem from the three dimensional graphite, invented in 1777 by Scheele.

Graphene, or more precisely monolayer graphene, is a one-atom thick two-dimensional (2D) structure of carbon atoms arranged in a honeycomb lattice with carbon- carbon bond length of about 0.142 nm. The three dimensional parent structure graphite, from where graphene originates, can be considered as the three dimensional stacking of multilayers of graphene with an interplanar spacing of 0.335 nm. The history of graphene is marked with times of approval and disapproval ranging from 1947 to the huge surprise of the 2004 [1] when the possibility of the existence of free standing graphene was experimentally realized. When Wallace [2] in 1947 used the model of the 2D crystal arranged in a honeycomb lattice to solve the problems related to the band structure of graphite, and later in 1990, when the model was utilized for the band structure determination of carbon nanotubes [3], nobody realized that the free standing material realization of this model was waiting to be brought into limelight within a few years. Based on the famous Mermin-Wagner theorem [4], free-standing atomic planes cannot exist naturally because of the thermo dynamical instability on the nanometer scale and, if

unsupported, they have a tendency to crumble and form disordered aggregates. In other words, naturally occurring free standing 2D crystals cannot be formed spontaneously because such crystals are thermodynamically unstable [5]. Deeper perception on this theory shows that its validity is confined to infinite systems and hence it is possible to realize finite sized 2D crystals in a perfectly ordered, long lived metastable state. Even though 2D crystals cannot be formed spontaneously, they can exist as stable structures when stacked and held together by van der Waals forces as part of any 3D structure like graphite. This was the breakthrough accomplished by the Manchester team in 2004, under the leadership of Andre Geim, when it was realized that graphene, a one- atom thick, two dimensional crystal of carbon atoms, or more specifically, a single planar sheet of sp^2 bonded carbon atoms, densely packed in a honeycomb crystal lattice, could be isolated from the bonding of its parental three dimensional structure, graphite, by a simple mechanical exfoliation process using Scotch tape [6–8]. The integrity of the 2D layer structure during the exfoliation process is kept well by the robust covalent bonds within the layer which are much stronger than the comparatively weaker van der Waals force between the layers in graphite. The Manchester group also demonstrated that the exfoliated graphene layer can either be supported on any suitable substrate or suspended from a supporting structure [9, 10]. The observation that, through graphene sheets, electrons can travel sub-micrometer distances without scattering, establishes the excitingly high mobility of these electrons and the excellent two dimensional crystal quality of graphene [11]. Here, there is an incompatibility when one considers the theoretical and experimental observation that perfect two-dimensional crystals cannot exist in the free state. Still, one can argue that the graphene structures form either an integral part of larger three-dimensional structures like the embedding graphite matrix or the supporting bulk substrates [12]. Recent transmission electron microscopy studies on suspended one atom thick graphene sheets, exhibiting long range crystalline order, provide experimental footing to the argument that these suspended graphene sheets are not perfectly flat. They exhibit intrinsic microscopic roughening on the scale of 1 nm and these observed corrugations in the third dimension could be quite significant in the stability of these two dimensional crystals [12].

The exciting electronic and structural characteristics of graphene, identified soon after its isolation, released an unparalleled surge of worldwide scientific curiosity, invoking the need for the integration of various scientific disciplines for more dedicated future work to unveil the hidden surprises this new material has yet to offer. When Andre Geim and Konstantin Novoselov of the Manchester University had their memorable achievement of winning the 2010 Nobel Prize in Physics for their innovative experiments regarding the two-dimensional material graphene, the spirit gave wings to the already vibrant scenario of graphene research to venture into the fields of developing the so called ‘all carbon-based devices’ with prospects to dominate the next generation device technology.

2 Graphene

High quality graphene is very strong, light, quite transparent and an excellent conductor of heat and electricity and is a highly sought after material as a transparent conductor for a variety of optoelectronic device applications. Graphene can be genuinely described as the most perfect 2D electronic material possible in nature [12], by virtue of the fact that the system is one atomic monolayer thick and charge carrier transport is confined in the 2D layer. The miraculous electronic properties of graphene can be attributed to the hexagonal honeycomb lattice network of carbons, in which each carbon atom is bonded to its three neighbors by strong σ bonds and the delocalized π electrons determine the low energy electronic structure. This lattice of graphene with two carbon atoms per unit cell (A and B) and the two triangular sublattices A and B indicated in different colors is shown in Fig. 1. The unit cell of graphene encompasses two π orbitals which form the bonding (π) and anti- bonding (π^*) states and give rise to a rather unique band structure that was first introduced by Walace in 1947 and is illustrated in Fig. 2. In analogy with conventional semiconductors, the π states form the lower energy valence band and the π^* states, the higher energy conduction band. The valence and conduction bands touch at six points, termed as the Dirac or neutrality points. Considering the inherent symmetry properties, these six points get reduced to a pair, K and K′, which are independent of one another. In fact, the Dirac points K and K′ correspond to the inequivalent corners of the Brillouin zone and are of much significance in the transport properties of graphene. The Fermi surface in graphene consists of the two K and K′ points in the Brillouin zone where the π and π^* bands cross. Since the orthogonal π and π^* states do not interact their crossing is allowed, and the π electrons in graphene provide an

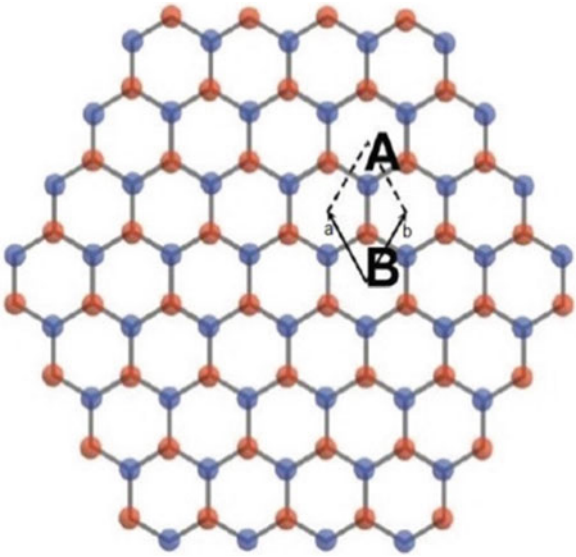

Fig. 1 The hexagonal honeycomb lattice of graphene, with two atoms *A* and *B* per unit cell. The underlying *triangular* Bravais lattice with lattice vectors **a** and **b** is also illustrated. Adapted with permission from [13]. Copyright ©2010 American Chemical Society

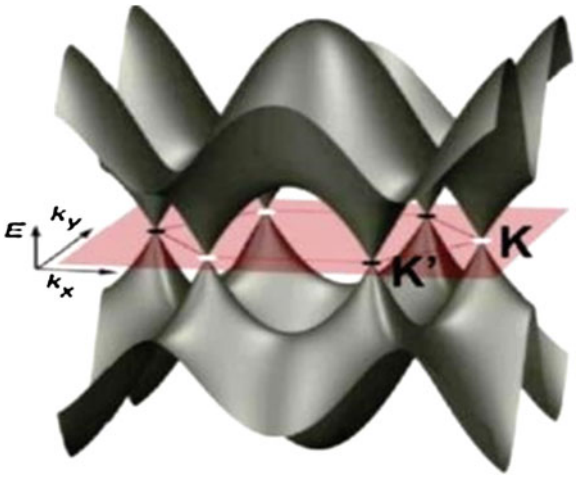

Fig. 2 The energy band structure of graphene showing the six Dirac points and the two inequivalent points K and K′. Adapted with permission from [13]. Copyright ©2010 American Chemical Society

ideal 2D system where one can realize the non-interacting π and π^* states within a single atom thick planar layer [13].

The π (bonding) and π^*(anti-bonding) bands have a linear (conical) dispersion at low energies and the band structure can be visualized as two cones touching at the Dirac point as shown in Fig. 3. Such a band structure has been shown to be quite receptive to modifications by suitable functionalizing and doping procedures. In view of the fact that the valence and conduction bands touch at the Dirac points, and based on the ambipolar nature of charge carriers (both electrons and holes), pristine graphene is considered as a zero band gap semiconductor [14–16].

The most striking aspect of graphene's energy dispersion is its linear energy momentum relationship with the conduction and valence bands intersecting at the Dirac point, corresponding to the wave vector q = 0, with zero energy gap. Graphene represents a zero band-gap semiconductor with a linear, energy dispersion for both electrons and holes, quite different from the parabolic energy dispersion

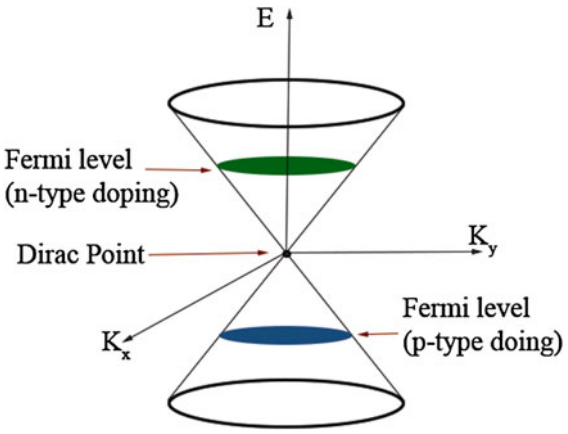

Fig. 3 The conical band structure of graphene, with the two cones touching at the Dirac point. Adapted with permission from [13]. Copyright ©2010 American Chemical Society

characteristic exhibited by other classes of well-studied two dimensional semiconductors including heterostructures, quantum wells and inversion layers. The band structure is symmetric about the Dirac point and hence the electrons and holes in pure, free-standing graphene should have similar properties. In fact, the electron and hole states in graphene are interconnected, exhibiting properties similar to the charge conjugation symmetry in quantum electrodynamics (QED).

Thus, at low energies, the presence of the two equivalent sublattices, A and B, in the structure of graphene allows the Hamiltonian to be written in the form of a relativistic Dirac Hamiltonian,

$$H = vF\sigma\hbar k \tag{1}$$

where v_F is the Fermi velocity of graphene, ħk the momentum vector measured from the Dirac point or K point and σ are Pauli spin matrices acting on the A and B sublattice degrees of freedom. In principle, the sublattice degree of freedom can be considered as an effective spin or a pseudo-spin which is parallel to the momentum vector in the conduction band and antiparallel to that in the valence band. This connection between the pseudo-spin and momentum in graphene sublattice is quite similar to that between real spin and momentum in Dirac equation [17].

The existence of two equivalent, but independent, sublattices A and B (corresponding to the two atoms per unit cell) gives rise to a novel chirality in graphene carrier transport properties. The two linear branches of graphene's conical energy dispersion intersecting at Dirac points, as shown in Fig. 4, are independent of each other and consequently are responsible for the origin of the pseudospin quantum number similar to electron spin, but completely independent of real spin. The carriers in graphene have a pseudospin index which can be represented by a spinor-like wave function in addition to the spin and orbital index. Akin to the situation in QED, the comparative contributions of the A and B sublattices in graphene are defined in terms of the spinor wave functions of the chiral pseudospin quantum number. However, in the case of graphene, the spin index specifies the sublattice rather than the real spin of the electrons.

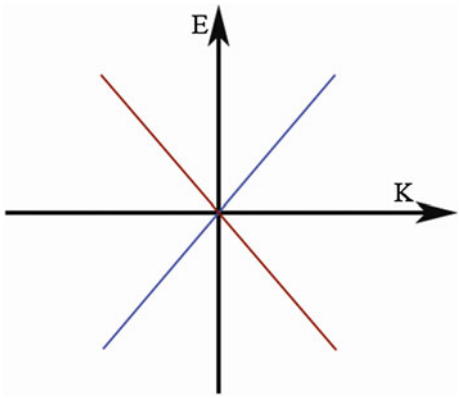

Fig. 4 The linear branches of the conical *E–K* plot of graphene. Adapted from [16]

At low energies, the energy-momentum relation (dispersion relation) in graphene is linear near the six corners (Dirac points) of the hexagonal Brillouin zone, which leads to zero effective mass for electrons and holes, in contrast to the massive parabolic dispersion behavior of conventional semiconductors. Electrons and holes near the Dirac points behave like relativistic particles which are quantum mechanically described by the massless Dirac equation for spin ½ particles and hence are termed Dirac fermions. It is quite interesting and exciting to see that in graphene the low-energy carrier dynamics can be well formulated in terms of massless, chiral, Dirac fermions. However, the Dirac fermions move with the Fermi velocity v_F, which is 300 times smaller than the velocity of light. A host of the unusual surprises of QED can hence be expected to show up in graphene but at much smaller velocities. Theoretically speaking, the most distinguishing feature of graphene, in addition to its strict 2D crystalline nature, is this exquisite, long wavelength, Dirac dispersion with a Fermi velocity close to 10^6 ms^{-1} [18, 19].

The unique band structure and the presence of charge carriers mimicking massless Dirac fermions have endowed graphene with exceptional carrier transport properties. Graphene combines both semiconductor and metal properties and hence offers prospects as a replacement for the currently used semiconductors in computer chips. It has thermal conductivity around ten times higher than that of common metals like copper and aluminum. The single atom thick two dimensional planar structure of graphene, representing a system with fewer atoms and much better thermal conductivity compared to many common metals, naturally should be much faster in electrical conduction. The electrons in graphene are found to travel faster by virtue of the much smaller effects of thermal vibrations on the conduction electrons in graphene, compared to many common metals and semiconductors. This could be the reason for the much smaller value of electrical resistivity in graphene, around 10^{-6} Ω-cm, which is about 35 % smaller than that of the lowest resistivity metal, silver, at room temperature. In suspended graphene, the limiting mobility at room temperature comes around 200,000 cm^2/Vs, which is more than twice that of the high mobility conventional semiconductors [20, 21]. At lower temperatures of around 240 K, carrier mobilities of up to 120,000 cm^2/Vs have been practically achieved in suspended graphene samples.

The charge carriers in graphene are endowed with the pseudospin, as mentioned earlier, and this aspect has much to do with the exceptionally high room temperature charge carrier mobility observed in graphene. The backscattering of charge carriers in graphene is suppressed, since the back scattering involves the reversing of the pseudospin of the charge carriers in addition to the momentum, which is not allowed for low energy defect states.

For graphene monolayers supported on substrates like silicon dioxide the mobility drops down to around 10,000 cm^2/Vs as a result of the transfer of electron vibration directly from the substrate to the graphene electrons. However, there is ample scope for improvement and the room temperature mobility of graphene supported on substrates can be significantly enhanced by working out procedures for choosing the right substrates devoid of atomic scale dirts and thus reducing the effects of scattering due to charged impurities and remote interfacial phonons.

The current carrying capacity of graphene is about 5×10^8 A/cm^2 which corresponds to about 1×10^{-6} A per atomic row of carbon, which is astonishingly high [22]. Graphene has astounding mechanical strength which is about 200 times greater than that of steel, mainly due to its robust network of sp^2 bonds while being stretchable and flexible at the same time [23]. Its thermal properties are also quite surprising, with extremely high thermal conductivity around 5,000 W/mK at room temperature, which is twenty times higher than that of copper. Its thermal expansion coefficient is large and negative which is of much significance in thermal stress management in graphene based devices. All these miraculous properties of graphene are highly favored for a variety of microelectronic device applications [17, 24]. As the thinnest material ever synthesized, the one atom thick graphene membranes are impermeable to even the lightest gas molecules and are the strongest and the stiffest among man-made materials.

In graphene one has the practical realization of two-dimensionality on an atomic length scale and this two-dimensionality is stronger in the sense that the electrons in graphene remain two dimensional up to room temperature and even up to the melting point of graphene. Pure graphene is a truly two dimensional metal even at room temperature and here one has the unique experience of elevating the two dimensional electron physics from its low temperature realms to the warmth of room temperature ambience.

It is an enticing experience to work with the group of phenomena that one encounters rarely in condensed matter physics, which are exclusively specified in terms of the fundamental constants and do not depend of material parameters. In this context, graphene has another magical offer to replenish the present awareness in many related phenomena, both from the theoretical and experimental viewpoints. The optical transparency of suspended graphene can be defined in terms of the fine structure constant, given by

$$\alpha = e^2/\hbar c \tag{2}$$

where e is the electronic charge, c is the velocity of light and h is the Planck's constant. The optical or dynamical conductivity G is generally used to express the optical properties of low dimensional structures like thin films. In the case of graphene exhibiting the conical dispersion relation of the zero rest mass Dirac fermions, the energy can be expressed as

$$\varepsilon = \hbar v_F |k| \tag{3}$$

where $\mathbf{k}$ is the wave vector and $\mathbf{v_F}$ is the Fermi velocity.

G has been theoretically predicted to have a universal value

$$G_0 = e^2/4\hbar \tag{4}$$

if the photon energy is much larger than the Fermi energy $\boldsymbol{\varepsilon_F}$. This universal value of G_0 indicates that all the three optical parameters of graphene, the transmittance T,

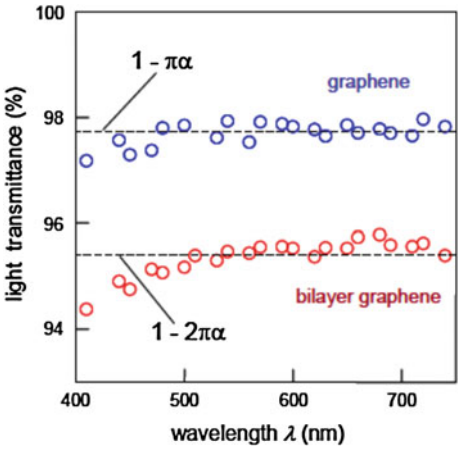

Fig. 5 Transmission spectrum of graphene, illustrating transmittance close to 98 % for monolayer graphene in the entire visible range. Adapted with permission from [24]. Copyright (2008) American Chemical Society

absorption A and the reflection R can be expressed in terms of fundamental constants. For normal incidence of light [25], the transmittance can be expressed as

$$T = (1 + 2\pi G_0/c)^{-2} \tag{5}$$

which on substitution of the value of G_0 can be approximated as $\approx 1 - \pi\alpha$.

Both R and T are explicitly related to G in the 2D case, which can be directly measured using graphene membranes. Here one has the exquisite experience of estimating the universal constant like G, using simple spectroscopic techniques, in the light of the unique electronic structure graphene can offer. Experimentally, G has been estimated to be close to $1.01G_0$ in the wavelength range from 450 to 800 nm and the corresponding transmittance T ≈ 97.7 %, which corresponds to an absorbance of about 2.3 % for graphene in this wavelength range [25, 26]. The transmittance spectrum of single layer and bilayer graphene is shown in Fig. 5. It can be seen that the transmittance decreases with the increase in the number of layers.

3 Graphene's Entry into Organic Optoelectronics

Graphene is a fascinating, truly two-dimensional material the present century has offered, whose electrons are confined to the two dimensional plane and exhibit characteristics akin to relativistic fermions. The extremely high charge carrier mobility, truly two dimensional crystalline order and the associated high electron mean free path, exceptionally high current carrying capacity, thermal conductivity, mechanical strength and flexibility and the high transparency over the entire visible range make it a highly preferred material for exotic applications in high speed electronics and flexible optoelectronics. The retention of the truly two dimensional

nature of electrons even at room temperature and above is the underlying factor, enriching the vast realm of its application prospects.

Single layer and multilayer graphene can be synthesized by a variety of techniques ranging from the mechanical exfoliation of graphite flakes, as illustrated by Geim and co-workers in their pioneering work in 2004 [1] to the more sophisticated techniques including epitaxial growth of large area graphene films on metal and semiconductor substrates [27] and the chemical vapor deposition of graphene on polycrystalline nickel and copper metallic substrates [28, 29]. The realms of two dimensional condensed matter electron physics have been made accessible to ordinary room temperature laboratories with the possibilities of graphene synthesis using mechanical exfoliation. This technique, however, has the disadvantage that the graphene sheets so generated are randomly placed without proper order. In order to utilize the prospects of graphene as an exotic electronic material for device applications, one has to resort to large area graphene synthesis on suitable substrates using more sophisticated techniques.

The central theme of the present chapter is to reflect upon the versatile role of graphene in realizing flexible organic photovoltaic devices with higher power conversion efficiency and long term stability. In general pristine graphene, being a zero gap semiconductor, cannot be utilized as is for device applications. A variety of doping, intercalation and striping schemes [30, 31] have been developed to open a band gap in pristine graphene and formulate band gap engineering procedures to tailor the band gap suitably for device fabrication. Methods have also been developed for introducing various functionalities by attaching suitable functional groups and moieties onto the graphene structure using both covalent and non-covalent approaches [32–39]. A very common and easily synthesized form of functionalized graphene is the graphene oxide (GO) which is bonded with a large number of hydroxyl, carboxyl and epoxy groups. It can be obtained by simply sonicating the graphite oxide, prepared by Hummers, Brodie or Staudenmaier methods [40], in organic or aqueous solvents [41,42]. Pristine, well defined graphene sheets (both single and multilayer) can be obtained by micromechanical or chemical exfoliation of graphite [1, 43] chemical vapor deposition (CVD) technique [44, 45] or by the reduction of graphene oxide (GO) by electrochemical, chemical or thermal means [46–48].

Graphene and its derivatives have emerged as the most promising materials for the building blocks of present-day optoelectronic devices by virtue of their stable yet tunable electronic and optical properties. Graphene can be tailor-made and functionalized to fit in various roles as required for a variety of applications; it can exist as highly conducting, semiconducting and insulating based on the number of layers, the type of functionalization, the type of doping and the type of morphologies. The use of graphene and its derivatives as window layers, transparent electrodes, hole transport layers, electron transport layers and active material has paved the way for developing a new category of stable and efficient organic photovoltaic devices.

Over the past three decades, organic photovoltaic cells have emerged as the third generation solar cells with quite advantageous prospects to dominate the power

generation industry in the near future. They are endowed with the inherent meritorious aspects of flexibility and cost-effective synthesis routes associated with organic molecules and polymers. The basic structure of an organic solar cell consists of the active material layer (donor + acceptor) capable of absorbing solar radiation sandwiched between the anode and the cathode, one of which has to be transparent enough to admit light transmission. In conventional type solar cells, the anode serves as the transparent electrode and in inverted type solar cells the cathode serves as the transparent electrode. Donor materials are usually low band gap polymers like poly (3-alkyl thiophenes) (P3AT) or organic molecules like the pthalocyanines, capable of efficient light harvesting [49–51].

Excitons are created, on light incidence on the donor material through the transparent electrode, which diffuse within the donor material and move towards the acceptor material. The strong electronegativity of the acceptor, combined with the built-in potential due to the work function difference between the two electrodes, results in effective carrier separation. Once the carriers are separated, they should be effectively transported to the electrodes to generate current in the external circuit. Suitable electron transport layers (ETL) and hole transport layers (HTL) are also necessary to get good power conversion efficiency (PCE) for the solar cell. In a typical solar cell, the anode is usually chosen as a transparent conducting material like indium tin oxide (ITO) which has a higher work function and the cathode is a metal like calcium or aluminum with a lower work function. In the earlier stages of development, organic solar cells generally had a bi-layer architecture represented by transparent anode/donor/acceptor/cathode as shown in Fig. 6a. The donor and acceptor materials in this structure remain as two separate layers sandwiched between the electrodes of dissimilar work function. Here, the thickness of the light absorbing donor layer is critical in such a way that the thickness should be of the order of the absorption length required for sufficient light absorption, which comes to about 100 nm. This thickness is quite high compared to the exciton diffusion length ($\sim$10 nm) in disordered organic semiconductors. Hence, it remained a big challenge to attain good power conversion efficiencies (PCE) until the introduction of bulk heterojunction (BHJ) concept in the 1990s. The BHJ concept [52, 53] could successfully address both the thickness requirements of the photoactive layer and the shorter exciton diffusion lengths. In these types of solar cells, the donor and acceptor materials interpenetrate each other forming a blend so that the interfaces between the donor and acceptor are spatially distributed as depicted in Fig. 6b. This can be achieved either by spin coating the donor-acceptor blend in the case of a polymer: polymer or polymer:organic small molecule active layer or by co-evaporation of conjugated molecules [52]. Further improvement in the solar cell characteristics has been achieved by introducing aligned (Fig. 6c) and non-aligned nanostructures, like zinc oxide nanorods, in the active layer, thereby improving the interfaces between the donor and acceptor layers [54–56]. The processability remains a difficult affair when inorganic nanomaterials are used as acceptor layers for fabricating solution processable solar cells. One of the best alternatives for nanostructured acceptor layer materials is graphene, which combines the flexibility and processability of polymers and the high mobility and thermal stability of the inorganic materials.

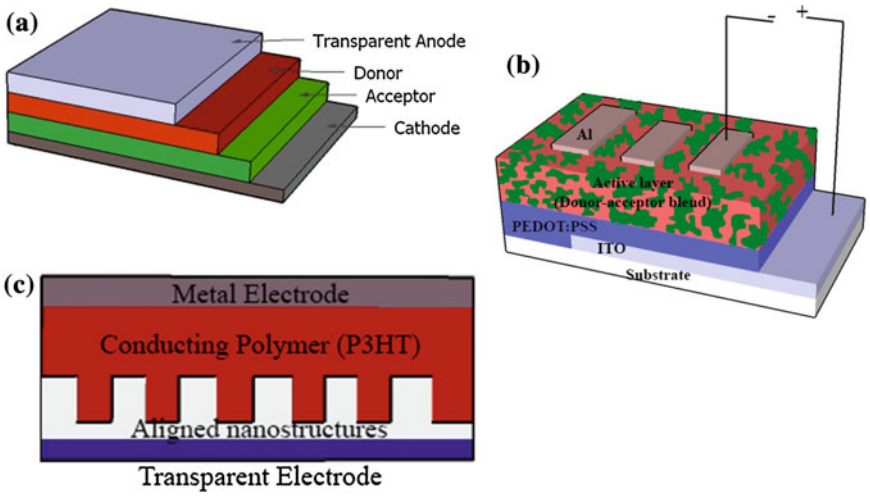

Fig. 6 Schematic of **a** planar heterojunction, **b** BHJ and **c** BHJ with aligned nanostructures

The enthralling features of graphene open the possibilities of its applications in versatile roles as the transparent conductive electrode, the hole transport layer (HTL), the electron transport layer (ETL) and the donor and acceptor layers to fabricate efficient, cost-effective, flexible and stable organic photovoltaic devices.

4 Graphene's Versatile Roles

The highly transparent graphene thin films are viable alternatives for the brittle and costly indium tin oxide (ITO) layers used in most of the optoelectronic devices. Pristine single layer graphene sheets obtained by mechanical exfoliation [57] exhibit a transmittance of about 97.7 % in the visible range and thus it absorbs only 2.3 % of the incident light. Pristine graphene has a typical work function of 4.4–4.5 eV which is very close to the highest occupied molecular orbitals (HOMO) of most of the p-type organic small molecules and polymers. This enables an effective and faster charge transfer between graphene and the organic molecules/polymers. The very high transparency, suitable work function, high electrical conductivity comparable to common metals and charge carrier mobility close to 10^5 cm^2/Vs have motivated many research groups to use graphene as the transparent conducting electrode instead of ITO in organic solar cells and obtained efficiencies comparable to that of ITO based ones [58]. It has been observed that the fill-factor of ITO-based solar cells fabricated on flexible substrates like polyethylene terephthalate (PET) drops to zero on bending the cell from 0°–60° whereas the CVD (chemical vapor deposition) graphene-based flexible OPVs are found to show negligible variation when bent up to 138°. The SEM analysis of the bent CVD

graphene and ITO sheets on flexible substrates provides sufficient evidence of the crack-free nature of graphene sheets compared to the micro-crack embedded morphology of the bent ITO sheets [59]. This result is quite significant in realizing flexible photovoltaic devices without compromising the efficiency and stability. The organic solar cells fabricated on multilayer films of graphene as electrodes with 84.2 % transparency are found to give a fill-factor (FF) of 32.6 % and power conversion efficiency (PCE) of 1.17 % [60]. On comparison with the PCE of 3.43 % obtained with ITO-based cells, although the PCE is smaller for the graphene based cells, they have the advantages of low cost and flexibility. In practice, the lower conductivity of the graphene sheets compared with that of ITO films is one of the major issues affecting the overall efficiency of the fabricated devices. This challenge can be met by using doped CVD grown graphene as transparent electrodes in organic solar cells and the PCE values of these devices are found to be comparable to their counterparts with ITO electrodes [61]. Another method to improve the conductivity of graphene is to use layer-by-layer molecular doping of graphene with p-type materials like the tetracyanoquinodimethane (TCNQ) [62]. Sandwiched graphene/TCNQ films stacked structure has been used as an anode in polymer solar cells with a poly (3-hexylthiphene) (P3HT): Phenyl-C61-butyric acid methyl ester (PCBM) active layer. Among these, the cells constructed with multilayer anodes with 2 TCNQ layers sandwiched by 3 graphene layers are found to give the maximum PCE of $\sim$2.58 % which is quite higher than that of devices with acid-doped multilayer graphene as the transparent anode.

Another major issue with pristine graphene electrodes is the poor surface wetting with many of the hole transporting layers like PEDOT:PSS which makes pristine graphene-based photovoltaic devices inferior to the ITO-based devices in their overall performance. This problem has been resolved by doping the graphene layer using $AuCl_3$ which can alter the surface wetting properties and enable the formation of a uniform coating of hole transporting layer over it. Other metal chlorides like $IrCl_3$, $MoCl_3$, $OsCl_3$, $PdCl_2$ and $RhCl_3$ have been used to dope CVD-grown graphene sheets and an increase in work function has been observed with increase in dopant concentration due to spontaneous charge transfer from the specific energy level of graphene to the metal ions [63]. The sheet resistance and transmittance are found to decrease with increase in dopant concentration. From these studies, $RhCl_3$ has been identified to be the strongest p-dopant and doping with this metal chloride and modifies the work function of graphene from 4.2 to 5.14 eV. This doping method also improves the overall conductivity of the graphene electrode thereby shifting the work function of graphene to desired values which further improves the PCE values [61].

Transition metal oxides like MoO_3 have also been successfully used to address the surface immiscibility issues between graphene sheets and PEDOT:PSS layer [64]. The bonding between PEDOT:PSS and graphene improves considerably as a result of this modification. It has been inferred that surface wettability plays an important role in improving the overall device performance. A detailed study on the effect of graphene morphology, the various combinations of hole transport layers and counter electrodes on the PCE and stability has also been performed to give a

better understanding in utilizing graphene as anode in organic solar cells. A significant increase in PCE has been obtained in the devices assembled using MoO_3 modified graphene as the transparent electrode [64].

Low-pressure chemical vapor deposited graphene layers with improved surface wettability have been introduced as a replacement for the ITO electrode in organic solar cells using a 15 nm PEDOT film as the hole transport layer on the graphene surface. In conventional methods, spin coated PEDOT:PSS films are used as the HTLs which have the disadvantages of poor surface wettability with graphene sheets, lower charge mobility compared to the PEDOT films and poor uniformity in thin film form. To avoid these issues between PEDOT:PSS and graphene layer, the very sophisticated vapor printing method, which includes shadow masking in combination with oxidative chemical vapor deposition (oCVD), has been used to get a very uniform, smooth, complete and pure PEDOT layer. This method yields organic photovoltaic devices of graphene/vapour printed PEDOT/DBP (tetraphenyldibenzoperiflanthene)/C_{60} (fullerene)/BCP (bathocuproine)/Al (aluminum) architecture having comparable efficiencies with the ITO based devices [65].

Another drawback of using pristine graphene as electrodes in photovoltaic applications is the significant reduction in the open circuit voltage when compared to the devices based on conventional semiconductors [66]. This problem is usually rectified by introducing a band gap in graphene and tailoring the Fermi level. Tailoring the optical and electrical properties of graphene can be achieved basically through four methods: (a) chemical modification (b) electrostatic field tuning, (c) hetero atom doping and (d) formation of graphene nanoribbons [66, 67]. Chemical modification of graphene can be done either by attaching various functional groups or by grafting organic small molecules/polymers to the graphene edges or basal planes [67]. These processes will introduce a band gap as well as modify the optical properties due to the introduction of new bands in the electronic structure of the obtained hybrid materials. The attached structures, or molecules, and the chemistry used determine the band gap and associated electrical and optical properties of the modified graphene.

Even though, pristine graphene sheets as such are not very promising as transparent electrodes in organic photovoltaic cells using polymers as the HTLs and polymer/organic small molecules as the active layers, in a recent study, 4–5 layers of graphene have been used as the transparent conductive electrodes for fabricating hybrid hetero junction solar cells based on silicon nanostructures and P3HT in which the PCE has attained values as high as 9.94 and 10.34 % [68]. Among the silicon nanostructures used, silicon nanohole arrays based cells show the highest PCE values (10.34 %) when compared to those cells based on silicon nanowire arrays (9.94 %) due to larger surface area offered and better support to graphene without dropping the capability of light absorption. The cell parameters, investigated by replacing graphene with metallic electrodes, are found to be comparatively inferior. The very high PCE values in these cells can be attributed to the efficient suppression of charge recombination and improved light harvesting capability of the graphene/silicon nanostructure combinations with P3HT. Interestingly, it has been found that solar cells with 5 layered-graphene electrodes out-perform those

cells with metallic electrodes due to the higher optical transparency of graphene over the metallic films.

Interfacial/buffer layers are used to match the work function and energy levels between subsequent layers in organic photovoltaic devices. The use of interfacial layers enables efficient charge separation that results in excellent power conversion efficiencies. Graphene oxide (GO) can be used as the anode interfacial layer in organic bulk heterojunction solar cells with ITO as the transparent electrode. Solution processed GO, nickel oxide (NiO) and GO/NiO bi-layers have been used as anode interfacial layers in bulk heterojunction organic solar cells which exhibit excellent PCE and fill factor values [69]. Of these, ITO/GO/NiO/P3HT:PCBM/LiF/Al devices are found to be the best, having cell efficiency of 3.48 % with the J_{SC} of 8.71 mA/cm$_2$, V_{OC} of 0.602 V and FF of 66.44 % (Fig. 7, Table 1). These enhanced cell parameters have been attributed to the well-matched energy levels between the various layers of the device, achieved as a result of the incorporation of GO/NiO bilayer. A 49 % improvement in efficiency has been achieved in these devices when compared to the corresponding devices without the interfacial GO layer, which acts as the hole transporting layer.

In a recent innovative approach, GO has been used as the interfacial layer with ITO electrode and aluminum doped zinc oxide (AZO) cathode buffer layer to improve the PCE values of conventional and inverted type solar cells [70]. A remarkable improvement in the solar cell parameters has been observed in the

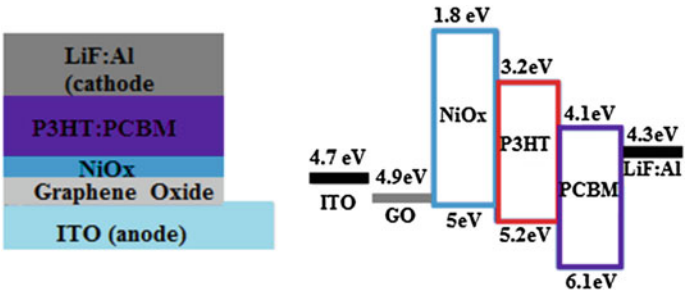

Fig. 7 Schematic of the GO/NiO_x bilayer solar cell and the corresponding band diagram. Reprinted from [69]. Copyright (2011), with permission from Elsevier

Table 1 Solar cell parameters of various devices with different combinations of HTLs

HTL configuration	J_{SC} (mA/cm^2)	V_{OC} (V)	FF (%)	PCE (%)
Without HTL	8.65	0.520	51.76	2.33
GO	8.85	0.565	54.94	2.75
Nickel oxide	9.08	0.604	56.58	3.10
GO/Nickel oxide	8.71	0.602	66.44	3.48
Nickel oxide/GO	9.11	0.602	54.91	3.01

Reprinted from [69]. Copyright (2011), with permission from Elsevier

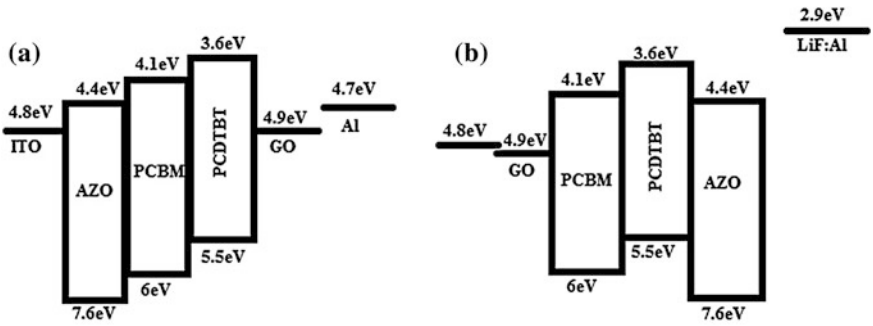

Fig. 8 Band diagrams of **a** inverted and **b** conventional type solar cells. Reprinted from [70]. Copyright (2012), with permission from Elsevier

inverted type cells. Inverted solar cells fabricated using solution processed AZO and tri-layer GO as cathode and anode buffer layers, the polymers PCDTBT, PBDTTPD as electron donors and PCBM as acceptor, are found to exhibit open-circuit voltages of 0.74 and 0.70 V, short-circuit current densities of −12.09 and −12.06 mA/cm2, fill factors (FFs) of 60.73 and 60.03 %, with overall power conversion efficiencies of about 5.46 and 5.07 %, respectively (Fig. 8). These values are quite higher compared to their conventional analogues as shown in Table 2.

The stability of thin film organic photovoltaic devices depends on the thermal and environmental stabilities of each layers used in the cell. The inhomogeneous electrical properties, high acidity suspension and hygroscopic properties of the commonly used PEDOT:PSS are some of the other major issues which affect the long term stability of the organic cells. A method to overcome these issues is to use graphene-based hole transport layers (HTL) instead of PEDOT:PSS. Improved stability has been observed in organic photovoltaic cells fabricated using UV/ozone treated graphene sheets instead of PEDOT:PSS as hole extraction or hole transporting layers. In such cells, comparable efficiencies with that of PEDOT:PSS based cells has been observed and the cells are capable of withstanding humid conditions up to 26 h of continuous working [71]. There has been a drastic decrease in the

Table 2 Solar cell parameters of conventional and inverted type solar cells using GO as anode interfacial layer and AZO as the cathode buffer layer

Device architecture	J_{sc} (mA/cm^2)	V_{oc} (V)	FF (%)	PCE average (%)
ITO/AZO/PCDTBT:PCBM/GO/Al	12.09	0.74	60.73	5.46
ITO/AZO/PBDTTPD:PCBM/GO/Al	12.06	0.7	60.03	5.07
ITO/GO/PCDTBT:PCBM/AZO/LiF:Al	7.18	0.65	60.01	2.81
ITO/GO/PBDTTPD:PCBM/AZO/LiF:Al	7.18	0.6	56.12	2.41

Reprinted from [70]. Copyright (2012), with permission from Elsevier

efficiency of PEDOT:PSS based devices which are found to work for only 14 h on exposure to the same humid atmosphere. There are also many other advantages of using UV/ozone treated graphene sheets instead of GO and reduced GO (r-GO) sheets as HTLs. The major disadvantage of using GO is the thickness of the layer, which, if higher, can make the GO layer more insulating and can affect adversely the overall efficiency of the cell. It is also very difficult to get proper band alignment with the various active layers when r-GO is used as the HEL.

The application of modified graphene is not limited to the transparent anode and the hole transporting layers in organic solar cells. It can also be used as efficient transparent cathode material as reported by a few research groups. The higher sheet resistance of the graphene layer, when compared with the conventional cathode materials, poses a major difficulty in overcoming the PCE values offered by the conventional cells. It has been reported that single layer graphene can be used as cathode material and the performance of the cell can be made much better if contact doping can be induced in the graphene layer, which reduces the sheet resistance considerably. The high transparency of the graphene also adds to the improvement in performance [72] (Fig. 9). Single layer graphene has been found to exhibit a very interesting property by which its work function can be made tunable when kept in contact with strong electron donating materials, which is a consequence of graphene's small density of states around the Dirac point. This process is termed as contact doping of graphene, since the contact with suitable electron donors

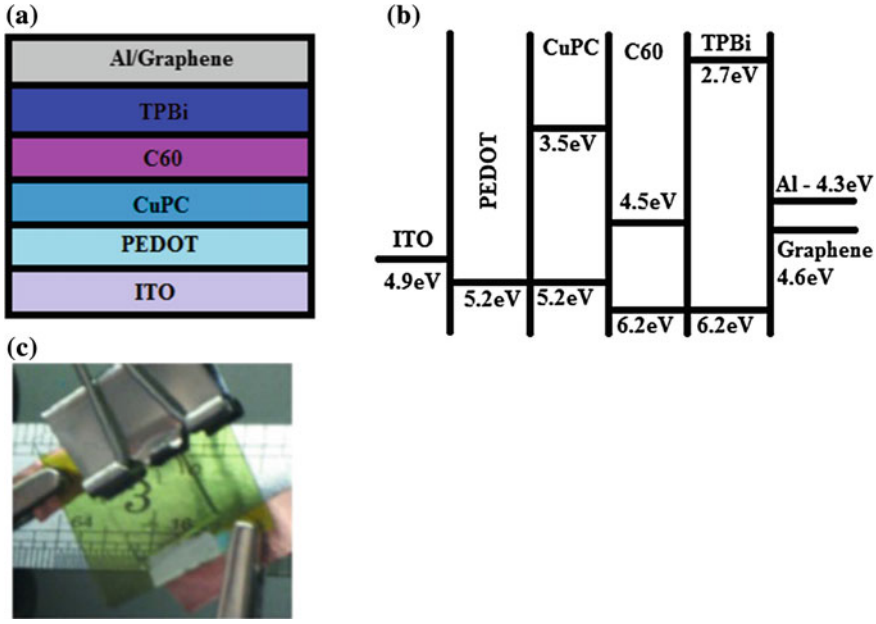

Fig. 9 **a** Device architecture of organic solar cells with graphene cathode, **b** band diagram of the device with graphene cathode and **c** photograph of the transparent devices with graphene cathode. Reprinted with permission from [72]. Copyright [2011], AIP Publishing LLC

facilitates work function tuning [73–75]. These studies highlight the possibility of using graphene as both cathode and anode materials in metal-free, flexible and light-weight, all-organic solar cells.

The major challenges for using graphene as cathode materials are concerned with achieving the required surface wettability, work function tuning and carrier transport. These issues can be solved to some extent by incorporating Al-TiO_2 nanocomposite to modify the single layer graphene [76]. The evaporated aluminum nanoclusters deposited on graphene improve the surface wettability for the subsequent deposition of TiO_2 in the composite, thereby reducing the work function of graphene to suit the energy levels. The solution processed TiO_2 being a good electron transporter helps graphene to extract charges more efficiently, thereby enhancing the overall efficiency of the solar cell. The self-assembly method adopted to deposit TiO_2 on the aluminum coated graphene offers better charge extraction when compared to the conventional spin coating process, which results in non-aligned structures. The main advantages of the self-assembly method are excellent uniformity and thickness control. The inverted organic solar cells with Al-TiO_2 modified graphene cathode exhibit twice the PCE values (2.58 %) compared to those with un-modified graphene cathodes (Fig. 10, Table 3). The PCE values of these organic solar cells have reached almost 75 % of those made using indium tin oxide.

In a recent study, graphene mesh transparent electrodes, prepared by photolithography and O_2 plasma etching, have been used as one of the transparent, conducting electrodes for organic bulk hetero junction solar cells with a power conversion efficiency of 2.04 % [77]. This is one of the highest PCE values for an organic solar cell based on solution-processed graphene electrode. A blend of poly (3-hexylthiophene) and phenyl-C_{61}-butyric acid methyl ester ($PC_{61}BM$) has been used as the active layer for this solar cell. The O_2 plasma treatment improves the hydrophilic nature of the graphene mesh and aids in the formation of uniform films on the PEDOT:PSS layer. This improved hydrophilicity is due to the introduction of some oxygen containing functional groups on the graphene surface.

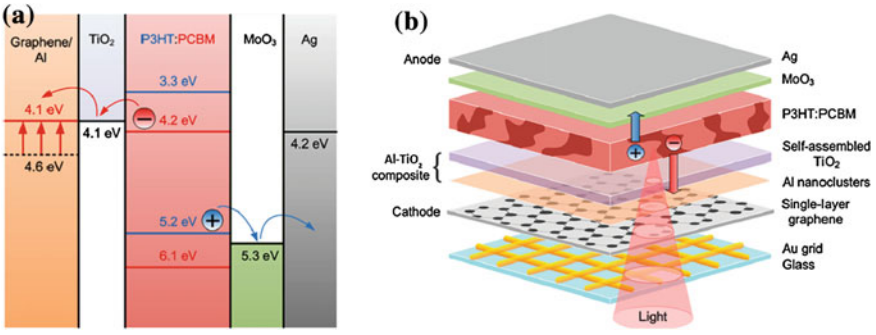

Fig. 10 **a** Band diagram of Al-TiO_2 modified, graphene based organic photovoltaic devices and **b** Architecture of device with graphene cathode. Adapted with permission from [76]. Copyright ©2013 American Chemical Society

Table 3 Device characteristics of inverted type polymer solar cells with Cathode/P3HT:$PC_{61}BM$/MoO_3/Ag architecture

Cathode	J_{SC} (mA/cm^2)	V_{OC} (V)	FF (%)	PCE (%)
SLG/Al-TiO_2	7.85 ± 0.24	0.58 ± 0.02	35.0 ± 3.2	1.59 ± 0.08
Grid/SLG/Al-TiO_2	8.55 ± 0.62	0.60 ± 0.01	50.1 ± 2.5	2.58 ± 0.09
ITO/Al-TiO_2	9.11 ± 0.25	0.63 ± 0.00	60.1 ± 0.3	3.45 ± 0.09
SLG/Al/spin-coated TiO_2	1.80 ± 0.65	0.30 ± 0.04	25.2 ± 0.5	0.14 ± 0.07
Grid only/Al-TiO_2	1.31 ± 0.56	0.61 ± 0.01	33.2 ± 0.5	0.27 ± 0.11

SLG single layer graphene

Adapted with permission from [76]. Copyright ©2013 American Chemical Society

5 Functionalization of Graphene

Functionalization of nanostructured materials refers to the attachment of functional groups at desired sites for suitable modification of the material characteristics. It is possible to design materials with tailor-made properties by adopting the most appropriate functionalization procedures.

The basal plane of graphene is comprised of strong covalent bonds of the sp^2 hybridized carbon atoms, whereas the edge sites contain dangling bonds and are comparatively more reactive. These dangling bonds at the edge sites are quite appropriate for covalently attaching different types of functional groups and molecules to achieve better processability, solubility, film forming properties and reactivity suitable for the desired type of chemical modifications. The graphene basal plane can also be covalently or non-covalently functionalized to impart modifications as required.

Functionalization of graphene in the basal planes and edges are excellent methods to design efficient hole and electron extraction materials with proper energy level matching with the various layers in organic energy harvesters. Edge functionalization of graphene can be used to synthesize cesium-neutralized graphene oxide (GO-Cs) by effecting charge neutralization of the –COOH groups attached to the periphery of GO with Cs_2CO_3 and the process is illustrated in Fig. 11a. The work function of GO gets modified upon this functionalization and GO-Cs has been identified to be a very good electron transporting material [78]. It is quite interesting to see that GO and GO-Cs can be used, respectively, as hole and electron extraction layers in conventional and inverted types of organic solar cells with a blend of P3HT and PCBM as the active layers [78–80]. These solar cells, with device architectures as depicted in Fig. 11b, c exhibit PCE values as high as 3.67 % and outclass the analogous conventional type BHJs with state-of-art hole and electron extraction layers. Recent research in edge functionalization of graphene has provided highly promising and effective ways to get functionalized graphene with controlled work function and optical properties with high prospects of improving the efficiency of organic solar cells [79–82].

Polymer solar cells with appreciable efficiency have also been realized based on basal-plane functionalized sulphated graphene oxide, GO-OSO_3H with a remarkable

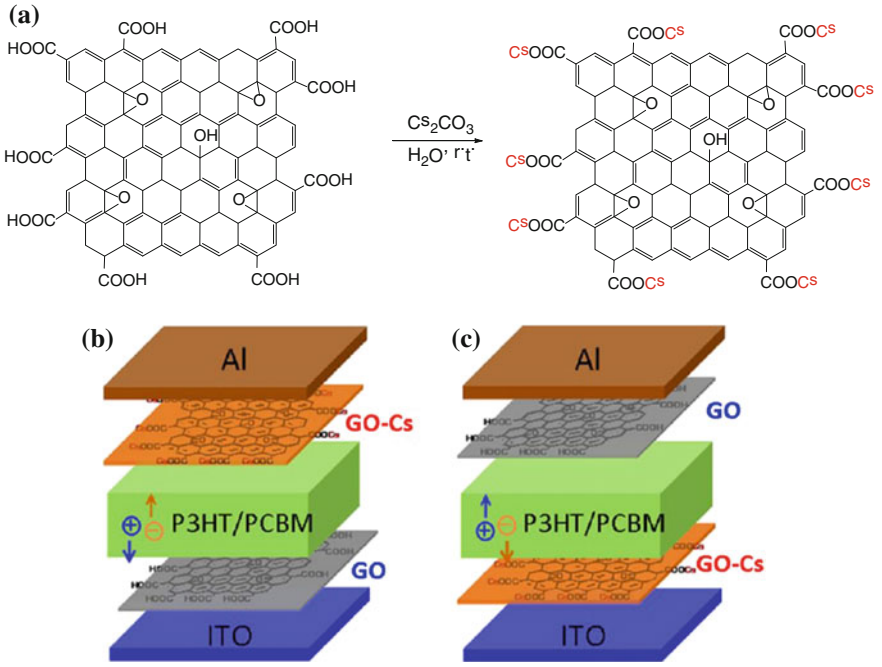

Fig. 11 **a** Synthesis route for Cs functionalization and **b**, **c** architecture of devices with edge functionalized GO as ETL. Adapted with permission from [79]. Copyright ©2013 American Chemical Society)

PCE of 4.37 % which is amongst the highest values obtained for solar cells with P3HT:PCBM active layers. Sulphated graphene oxide can be synthesized by substituting the hydroxyl or the epoxy groups of the carbon basal plane of graphene oxide (GO) with $–OSO_3H$ groups, by treating with fuming sulphuric acid, while keeping its –COOH edge groups intact, as illustrated in Fig. 12. The sulphated graphene oxide functions as the hole extraction material in this polymer solar cell which exhibits excellent performance characteristics [80].

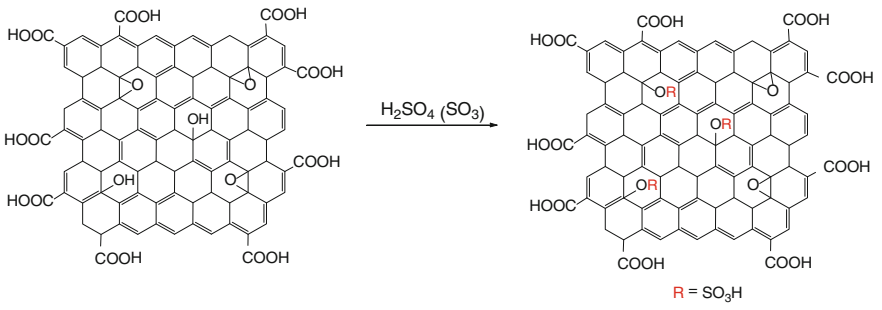

Fig. 12 The synthesis route for GO-OSO_3H

Graphene based acceptor layers can be used to improve the efficiency and thermal stability of organic/hybrid bulk hetero junction solar cells. Several modifications on the graphene surface have been adopted to improve the charge transport and separation in solar cells. The fullerene based acceptors with very low stability can be replaced by these modified stable counterparts. An electron transporting material developed from hydrazine-reduced graphene oxide by a simple lithiation reaction has been found to yield a covalent attachment of monosubstituted C_{60} on the graphene sheet [83]. A 2.5 fold improvement in the PCE values has been observed in P3HT based solar cells when C_{60} is replaced by this electron acceptor due to enhanced electron transport or efficient carrier separation. The C_{60} grafted graphene sheet will be a very attractive inclusion for hybrid all-carbon devices.

Graphene quantum dots (GQDs) represent a new type of nanomaterials which have very unique and distinctive electrical and optical properties and are being widely investigated for a variety of applications. The GQDs can be synthesized by the very simple, cost-effective and high-yield hydrothermal method. Although graphene quantum dots are used in hybrid/organic solar cells as electron acceptors, the power conversion efficiencies of these cells are not very promising. Graphene quantum dots can be effectively used as cathode buffer additives with cesium carbonate (Cs_2CO_3) in bulk hetero junction inverted polymer solar cells and 22 % enhancement in the PCE values (2.59–3.17 %) has been observed, when compared to that with Cs_2CO_3 alone [84]. This can be attributed to the improved exciton dissociation and suppressed electron–hole recombination at the cathode-polymer active layer interface. In this architecture, depicted in Fig. 13, GQDs act as excellent electron transfer and hole blocking material (Table 4).

In most of the bulk hetero junction organic solar cells, fullerene and fullerene derivatives have become indispensable as the electron acceptors owing to the higher charge mobilities compared to the polymer-based acceptor molecules. The overall stability of the cell depends upon the thermal stability of the electron acceptors also and hence, it is desirable to replace fullerene and its derivatives with suitable

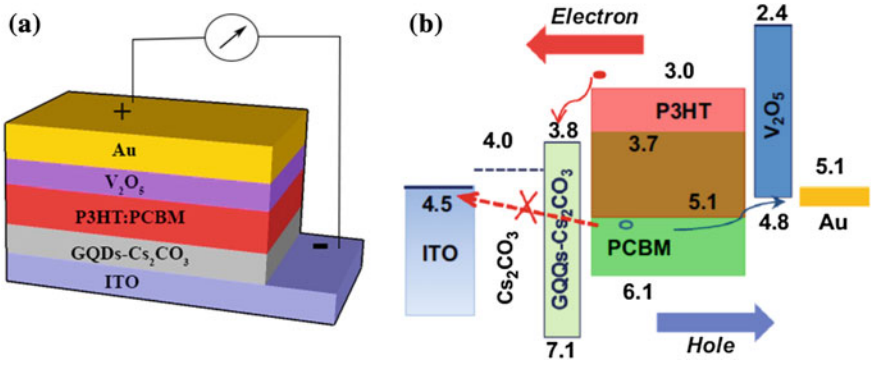

Fig. 13 **a** Device structure of the GQD based inverted organic solar cell and **b** Energy band diagram of inverted polymer solar cells with Cs_2CO_3 or GQDs-Cs_2CO_3 buffer layers. Reprinted from [84]. Copyright (2013), with permission from Elsevier

Table 4 Device characteristics of inverted organic solar cells with different cathode buffer layers

Cathode buffer	J_{SC} (mA/cm^2)	V_{OC} (V)	FF (%)	PCE (%)
GQDs	4.7	0.509	33.2	0.79
Cs_2CO_3	8.37	0.57	54.2	2.59
GQDs-Cs_2CO_3	9.04	0.585	60	3.17

Reprinted from [84]. Copyright (2013), with permission from Elsevier

materials with higher charge mobility and thermal stability. In a typical study, aqueous-dispersible graphene (a-dG) sheets have been presented as the substitutes for the acceptor materials that offer efficient charge transfer between the donor polymer, poly[3-(potassium-6-hexanoate) thiophene-2, 5-diyl] (P3KT) and the a-dG acceptor in a 'green' polymer solar cell with ITO/PEDOT:PSS/P3KT:a-dG/ZnO/Al architecture [85]. The a-dGs can be synthesized by reducing graphene sheets in the presence of the water soluble P3KT by non-covalent functionalization. An efficient charge transfer occurs between P3KT and a-dG, whose chemical structures are depicted in Fig. 14a, b. The charge transfer can be confirmed from the fluorescence quenching observed in P3KT due to the presence of a-dG. The performance of the a-dG modified polymer solar cell has also been found to be superior when compared to that of the one without a-dG in the P3KT film. This study has extended the role of graphene as excellent electron acceptors in easily processable, environmental friendly and low-cost polymer solar cells. In addition to the higher thermal stability and charge mobility, functionalized graphene has the advantages of low cost and ease of synthesis when compared to the other widely used organic acceptor materials.

Functionalized graphene blended with donor polymers such as P3HT has been used by many researchers as the active layer in their bulk hetero junction photovoltaic devices to enhance the stability and improve the charge separation. It has been observed that there is an optimal graphene content and a moderate annealing treatment is required to obtain the maximum efficiency out of the device.

The present PCE values of single bulk hetero junction (BHJ) photovoltaic devices have approached 9 % owing to the advances in the appropriate band gap tailoring and energy level modifications of the photo active layers and the controlled interface engineering strategies for efficient charge separation and collection by the electrodes [86–88]. The low charge carrier mobilities and narrow optical

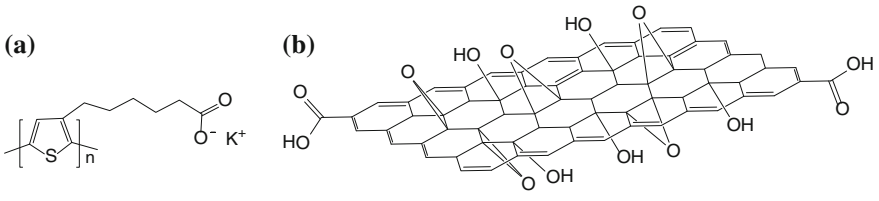

Fig. 14 Chemical structure of **a** P3KT and **b** a-dG

absorption band width associated with organic molecules and conjugated polymers are the prime challenges encountered for enhancing the PCE values well above 10 % for single junction devices [89–91]. The multi-junction or the tandem concept is a versatile approach to enhance the efficiency of photo voltaic devices, by which the harvest of a wide spectral solar radiation can be made viable. The solar radiation absorption window can be broadened by stacking together wide and low band gap photo active materials capable of light absorption over a much broader wavelength region. In the tandem solar cell configurations, where two or more sub-cells with matching light absorption are stacked and connected in series or parallel, PCE values above 10 % have been achieved [92, 93].

The adaptability of graphene has crossed another milestone with the realization that graphene can function effectively as the intermediate layer (IML) in tandem solar cells to boost the overall efficiency. In the tandem configuration with sub cells connected either in series or parallel, the IML should act as the protective layer between sub cells to prevent intermixing of any two sub cells. The material acting as the IML should also have quite high electrical conductivity and minimum light absorption. Compared to the series connected tandem cell, which does not demand stringent material perfection in terms of electrical conductivity and transmittance for the IML, the parallel connected tandem configuration is essentially in need of highly transparent and conductive IML without structural discontinuities. With most of the metallic IMLs the main hurdle is the light transmission loss close to 40 %, which can inhibit the light harvesting capability of the parallel tandem device [94]. Carbon nanotubes (CNTs), in spite of the high electrical conductivity are not suitable as efficient IML materials, owing to the large contact resistance between CNTs and the organic molecules [95]. In parallel connected tandem cells, any two sub cells can operate individually and higher efficiency can be achieved more easily, compared to the series connected tandem cells, and the demand for developing parallel connected tandem cells is on the soar all through the photovoltaic industry.

Graphene has recently been identified as a highly pursued material as the IML in both series and parallel connected tandem cells, owing to the excellent transparency and high electrical conductivity, combined with the possibility that the soft graphene membranes can be conveniently transferred to a variety of substrates, according to the requirement. Graphene films coated with MoO_3 offer high prospects as IMLs between each sub cell in tandem polymer (parallel and series configurations) solar cells and considerable improvement in the open circuit voltage and short circuit current values has been achieved [94]. The deposition of a MoO_3 layer of particular thickness over CVD grown graphene films modifies the work function of graphene layers to match with the energy levels of subsequent layers. It has also been found that the work function of graphene layers increases with the increase in thickness of MoO_3 layer; this offers the possibility to tune the work function of MoO_3 coated graphene layers, in terms of the MoO_3 layer thickness, to match with that of the layers in contact, to achieve efficient charge extraction. The work function of graphene interface has to be suitably controlled to minimize charge build- up between sub cells in tandem configuration. It has been established experimentally that graphene based IMLs are highly efficient in joining sub cells of

tandem cells so that the open circuit voltage and short circuit current density get multiplied, in proportion to the number of sub cells involved [94]. This is a new leap towards developing organic tandem cells with much pronounced thermal and environmental stability, efficiency, and design flexibility.

5.1 Towards All-Carbon Devices

Electric power generation from inorganic semiconductor based photovoltaic technology is still alarmingly expensive compared to fossil fuel technology, even when intense research is on the soar globally for identifying strategies towards cost reduction. A host of new materials have been developed over the past two decades as alternatives to replace silicon and gallium arsenide like expensive photoactive inorganic materials, which include conjugated polymers, organic small molecules and carbon-based nanostructures. These organic analogues with excellent light absorption and tunable electrical conductivity offer the possibility of assembling thin film structures on light weight and flexible substrates. The cost reduction can be genuinely realized by adopting roll to roll, large area device processing technology, employing cost effective techniques like solution processing or the methods based on paintable inks, at low temperatures and ambient pressure conditions, which are feasible with organic materials [96, 97]. Solution deposition based roll to roll processes can be suitably adapted to install organic photovoltaic devices on any types of surfaces without worrying about the shape constraints, on textiles, automobiles and buildings, so as to make solar cells affordable and accessible on a general basis. Although there is a long way to go for realizing these visions, the recent advances in carbon-based nanostructures are very promising to expect breathtaking giant leaps in this direction within the next 5–10 years.

Carbon, known from time immemorial, constitutes one of the most abundant materials on the Earth's crest and in tune with the widespread technological demand, is produced in huge quantities to the extent of 9 Giga tons per year [98]. Along with the naturally occurring graphite, diamond and coal, carbon nanotubes, fullerenes and graphene, which are the nanostructured carbon allotropes, are also being extensively utilized for many technological applications. These carbon nanostructures and their substituted derivatives and functionalized forms offer excellent prospects in terms of charge carrier mobility and optical absorption for organic photovoltaic applications. Both conducting and semiconducting properties can be envisaged in these carbon nanostructures based on their chemical structure and are the prime factors for their suitability to be used in combination to realize devices consisting entirely of carbon-based materials. Though carbon-based devices are in the infant state of development, there is high probability that the carbon-based photovoltaic devices may dominate the power industry, as the next generation cost effective solar cells, within the next decade. Such devices have many attractive features to offer, the most important one being the possibility of production at much cheaper rates and in large quantities due to the abundance and availability of

carbon. The carbon-based nanomaterials and their functionalized forms can be dispersed and also grown on suitable substrates using cost effective solution processes which makes their integration into roll to roll manufacturing processes highly feasible and scalable [99–101]. Many of the carbon-based active materials suitable for device fabrication are also endowed with unparalleled, long term temperature and chemical stability [102–104] which makes them highly sought after materials of the present century.

The recent surge of research enthusiasm towards carbon nanostructures has resulted in utilizing them as the transparent electrodes, interconnects, electron/hole transport layers, buffer layers [105] and as the acceptor layers in combination with conjugated polymers or small organic molecules as donor layers [96, 97] in organic photovoltaic devices. As the initial leap towards "all-carbon devices" attempts have been carried out to replace the conjugated polymers and small molecules with carbon nanostructures in combination, to function as the main active layer components, and bilayer photovoltaic devices with PCE values close to 0.85 % have been realized using fullerenes in combination with single walled carbon nanotubes (SWCNTs) or composites of SWCNTs with reduced graphene oxide (rGO) and fullerenes [106, 107]. Further modifications in device structure have resulted in efficiencies around 1.3 %, based on entirely solution deposited and carbon-based active layers consisting of semiconducting SWCNTs, the fullerene derivative PCBM and rGO in the bulk- heterojunction architecture [108]. The photo active layer is completely devoid of conjugated polymers or small molecules and the active layer consisting entirely of carbon nanomaterials provides atomic carbon concentration around 80–90 %, compared to the much lesser carbon concentration around 40–50 % in polymer based solar cells [108]. Carbon-based nanomaterials offer all the meritorious aspects of conjugated polymers and organic molecules including solution processability, chemical tunability and mechanical flexibility with the added benefits of much higher photo and thermal stability.

Although these advancements towards carbon-based photovoltaic devices are quite promising, these devices are not entirely carbon-based, and in these devices, indium tin oxide and silver/aluminum function as the anode and the cathode respectively. A breakthrough has been achieved [109] with the recent reports on the fabrication of the first, all-carbon photovoltaic device by Stanford University scientists, in which all the components are made entirely of carbon-based materials, including the anode, the active layer and the cathode. In this approach, the active layer consists of a bilayer film of solution processed and sorted semiconducting SWCNTs functioning as the light absorbing donor, and fullerene C_{60} as the acceptor, and reduced graphene oxide and doped (n-type) SWCNTs function respectively as the anode and the cathode [109]. This all-carbon solar cell has been found to have a PCE much less than 1 % for near infrared illumination. Although the PCE value is quite small for these all-carbon solar cells, there is ample scope for improvement. By suitably choosing the active layer components, especially the semiconducting SWCNTs, capable of light absorption in a broader range of the solar spectrum including the visible spectrum, the efficiency can be considerably improved. The use of unidirectionally aligned SWCNTs in the active layer can

significantly reduce the exciton trapping and enhance the exciton diffusion length and contribute towards achieving higher efficiency [109]. The Stanford research team is also working out strategies for using smoother and more conductive and more transparent, graphene based anode layer to facilitate better charge collection and achieve more incident light intensity. It is also equally challenging to directly deposit a much smoother SWCNT cathode film with better contact to the semiconducting SWCNT and C_{60} active layer without damaging the active layer which lies underneath to improve efficiency and device performance [109].

The dream of realizing all-carbon solar cells has already spread wings to conquer the heights of perfection. Though there is still a long way to go for this novel concept to flourish into marketable device technology, the ambience is all set for giant leaps towards miraculous achievements. Carbon-based materials are quite robust and are stable up to air temperatures around 1,100 °F. According to the Stanford research team working on all-carbon solar cells, the need for higher efficiency of these novel devices is balanced by the capability of these devices to outperform the conventional solar cells under extreme conditions of high temperature, pressure and physical stress. The manufacturing costs are also considerably reduced, since carbon materials can be coated on any substrate, employing solution deposition techniques, which do not require sophisticated and expensive machinery, contrary to the expensive processing technology of silicon-based devices. Considering the accessibility and abundance of carbon materials with potentials not yet utilized for energy harvesting technologies and the innovations emerging in material processing and device fabrication concepts, the future holds bright promises for the all-carbon photovoltaic devices. May be the days are not far away, to witness the flexible carbon solar cells adorning the surfaces and windows of buildings and automobiles, and generating electric power, in tune with the richness and simplicity of green chemistry.

References

1. Novoselov KS, Geim AK, Morozov SV, Jiang D, Zhang Y, Dubonos SV, Grigorieva IV, Firosov AA (2004) Science 306:666
2. Wallace PR (1947) Phys Rev 71:622
3. Ajiki H, Ando T (1993) J Phys Soc Jpn 62:1255
4. Mermin ND, Wagner H (1966) Phys Rev Lett 17:1133
5. Fasolino A, Los JH, Katsnelson MI (2007) Nat Mater 6:858
6. Geim AK (2009) Science 3:1530
7. Novoselov KS, Jiang D, Schedin F, Booth TJ, Khotkevich VV, Morozov SV, Geim AK (2005) Proc Natl Acad Sci USA 102:10451
8. Geim AK, Novoselov KS (2007) Nat Mater 6:183
9. Meyer JC, Geim AK, Katsnelson MI, Novoselov KS, Booth TJ, Roth S (2007) Nature 446:60
10. Blake P, Hill EW, Castro Neto AH, Novoselov KS, Jiang D, Yang R, Booth TJ, Geim AK (2007) Appl Phys Lett 91:063124
11. Meyer JC, Geim AK, Katsnelson MI, Novoselov KS, Booth TJ, Roth S (2007) Nature 446:60

12. Geim AK, MacDonald AH (2007) Phys Today 60:35
13. Avouris P (2010) Nano Lett 10:4285
14. Wilson M (2006) Phys Today 59:21
15. Castro Neto AHF, Guinea N, Peres MR, Novoselov KS, Geim AK (2009) Rev Mod Phys 81:109
16. Sharma SD, Shaffique A, Hwang EH, Rossi E (2011) Rev Mod Phys 83:407
17. Fuhrer MS, Lau CN, MacDonald AH (2010) MRS Bull 35:289
18. Novoselov KS, Geim AK, Morozov SV, Jiang D, Zhang Y, Katsnelson MI, Grigorieva IV, Dubonos SV, Firsov AA (2005) Nature 438:197
19. Zhang Y, Tan Y-W, Stormer HL, Kim P (2005) Nature 438:201
20. Chen JH, Jang C, Xiao SD, Ishigami M, Fuhrer MS (2008) Nat Nanotechnol 3:206
21. Morozov SV, Novoselov KS, Katsnelson MI, Schedin F, Elias DC, Jaszczak JA, Geim AK (2008) Phys Rev Lett 100:016602
22. Standley B, Bao W, Zhang H, Bruck J, Lau CN, Bockrath M (2008) Nano Lett 8:3345
23. Lee C, Wei XD, Kysar JW, Hone J (2008) Science 321:385
24. Balandin AA, Ghosh S, Bao W, Calizo I, Teweldebrhan D, Miao F, Lau CN (2008) Superior thermal conductivity of single-layer graphene. Nano Lett 8:902
25. Nair RR, Blake P, Grigorenko AN, Novoselov KS, Booth TJ, Stauber T, Peres NMR, Geim AK (2008) Science 320:1308
26. Sheehy DE, Schmalian J (2009) Phys Rev B 80:193411
27. Berger C, Song ZM, Li XB, Wu XS, Brown N, Naud C, Mayo D, Li TB, Hass J, Marchenkov AN, Conrad EH, First PN, de Heer WA (2006) Science 312:1191
28. Reina A, Jia XT, Ho J, Nezich D, Son HB, Bulovic V, Dresselhaus MS, Kong J (2009) Nano Lett 9:30
29. Li XS, Cai WW, An JH, Kim S, Nah J, Yang DX, Piner R, Velamakanni A, Jung I, Tutuc E, Banerjee SK, Colombo L, Ruoff RS (2009) Science 324:1312
30. Park J, Lee WH, Huh S, Sim SH, Kim SB, Cho K, Hong BH, Kim KS (2011) J Phys Chem Lett 2:841
31. Park J, Jo SB, Yu YJ, Kim Y, Yang JW, Lee WH, Kim HH, Hong BH, Kim P, Cho K, Kim KS (2012) Adv Mater 24:407
32. Sinitskii A, Dimiev A, Corley DA, Fursina AA, Kosynkin DV, Tour JM (2010) ACS Nano 4:1949
33. Hossain MZ, Walsh MA, Hersam MC (2010) J Am Chem Soc 132:15399
34. Nemes-Incze P, Osváth Z, Kamarás K, Biro LP (2008) Carbon 46:1435
35. He H, Gao C (2010) Chem Mater 22:5054
36. Liu Y, Zhou J, Zhang X, Liu Z, Wan X, Tian J, Wang T, Chen Y (2009) Carbon 47:3113
37. An X, Butler TW, Washington M, Nayak SK, Kar S (2011) ACS Nano 5:1003
38. Bai H, Xu Y, Zhao L, Li C, Shi G (2009) Chem Commun (13):1667 doi:10.1039/B821805F
39. Liu H, Gao J, Xue M, Zhu N, Zhang M, Cao T (2009) Langmuir 25:12006
40. Park S, Ruoff R S (2009) Nature Nanotech 4:217
41. Stankovich S, Piner RD, Chen X, Wu N, Nguyen ST, Ruoff RS (2006) J Mater Chem 16:155
42. Stankovich S, Dikin DA, Piner RD,Kohlhaas K A, Kleinhammes A, Jia Y, Wu Y, Nguyen S T, Ruoff R S(2007) Carbon 45:1558
43. Lotya M, Hernandez Y, King PJ, Smith RJ, Nicolosi V, Karlsson LS, Blighe FM, De S, Wang ZM, McGovern IT, Duesberg GS, Coleman JN (2009) J Am Chem Soc 131:3611
44. Kim KS, Zhao Y, Jang H, Lee SY, Kim JM, Kim KS, Ahn J-H, Kim P, Choi J-Y, Hong BH (2009) Nature 457:706
45. Li X, Cai W, An J, Kim S, Nah J, Yang D, Piner R, Velamakanni A, Jung I, Tutuc E, Banerjee SK, Colombo L, Ruoff RS (2009) Science 324:5932
46. Park S, Ruoff RS (2009) Nat Nanotechnol 4:217
47. Shao YY, Wang J, Engelhard M, Wang CM, Lin YH (2010) J Mater Chem 20:743
48. Zhu YW, Stoller MD, Cai WW, Velamakanni A, Piner RD, Chen D, Ruoff RS (2010) ACS Nano 4:1227

49. Kroon R, Lenes M, Hummelen JC, Blom PWM, De Boer B (2008) Polymer Rev 48:531
50. Vanlaekea P, Swinnenb A, Haeldermansb I, Vanhoylandb G, Aernoutsa T, Cheynsa D, Deibela C, D'Haena J, Heremansa P, Poortmansa J, Manca JV (2006) Sol Energ Mat Sol 90:2150
51. Yoon SM, Lou SJ, Loser S, Smith J, Chen LX, Facchetti A, Marks T (2012) Nano Lett 12:6315
52. Pagliaro M, Palmisano G, Ciriminna R (2008) Flexible solar cells. Wiley-VCH Verlag, GmbH & Co. KGaA, Weinheim, pp 85
53. Yu G, Gao J, Hummelen JC, Wudl F, Heeger AJ (1995) Science 270:1789
54. Liang Z, Gao R, Lan J-L, Wiranwetchayan O, Zhang Q, Li C, Cao G (2013) Sol Energ Mat Sol 117:34
55. Ahmadi M, Mirabbaszadeh K, Ketabch M (2013) Electron Mater Lett 9:729
56. Kang Y, Park N-G, Kim D (2005) Appl Phys Lett 86:113101
57. Wan X, Huang Y, Chen Y (2012) Acc Chem Res 45:598
58. Wang H-X et al (2013) Small 9:1266
59. Zhang Y, Zhang L, Zhou C (2013) Acc Chem Res 46:2329
60. Choi Y-Y et al (2012) Sol Energ Mat Sol 96:281
61. Park H et al (2010) Nanotechnology 21:505204 (6 p)
62. Hsu C-L (2012) ACS Nano 6:5031
63. Kwon KC et al (2012) Adv Funct Mater 22:4724
64. Park H et al (2012) Nano Lett 12:133
65. Park H et al (2012) ACS Nano 6:6370
66. Wang H-X (2013) Small 9:1266
67. Georgakilas V et al (2012) Chem Rev 112:6156
68. Yiming W et al (2013) J Phys Chem C 117:11968
69. Ryu MS and Jang J (2011) Sol Energy Mat Sol 95(10):2893
70. Yusoff ARBM et al (2012) Org Electron 13(11):2379
71. Kwon KC et al (2013) Sol Energy Mat Sol 109:148
72. Cox M et al (2011) Appl Phys Lett 98:123303
73. Ryu S, Brus LE, Kim KS, Kim P, Yu Y-J, Zhao Y (2009) ACS Nano 9:3430
74. Lee DS, Krauss B, Patthey L, von Klitzing K, Smet JH, Starke U, Coletti C, Riedl C (2010) Phys Rev B 81:235401
75. Rusu C, Brocks G, van den Brink J, Kelly PJ, Khomyakov PA, Giovannetti G (2009) Phys Rev B 79:195425
76. Zhang D et al (2013) ACS Nano 7:1740
77. Zhang Q, Wan X, Xing F, Huang L, Long G, Yi N, Ni1 W, Liu Z, Tian J, Chen Y (2013) Nano Res 6:478
78. Liu J, Xue Y, Gao Y, Yu D, Durstock M, Dai L (2012) Adv Mater 24:2227–2231
79. Dai L (2013) Acc Chem Res 46:31–42
80. Liu J, Xue Y, Dai L (2012) J Phys Chem Lett 3:1928
81. Jeon I-Y, Shin Y-R, Sohn G-J, Choi H-J, Bae S-Y, Mahmood J, Jung S-M, Seo J-M, Kim M-J, Chang DW, Dai L, Baek J-B (2012) Proc Natl Acad Sci USA 109:5588
82. Choi EK, Jeon IY, Bae SY, Lee HJ, Shin HS, Dai LM, Baek JB (2010) Chem Commun 46:6320
83. Yu DS, Park K, Durstock M, Dai LM (2011) J Phys Chem Lett 2:1113
84. Yang HB et al (2013) Sol Energy Mat Sol 117:214
85. Liu Z et al (2012) Sol Energy Mat Sol 97:28
86. Chen HY, Hou JH, Zhang SQ, Liang YY, Yang GW, Yang Y, Yu LP, Wu Y, Li G (2009) Nat Photonics 3:649
87. You JB, Li XH, Xie FX, Sha WEI, Kwong JHW, Li G, Choy WCH, Yang Y (2012) Adv Energy Mater 2:1203
88. Price SC, Stuart AC, Yang LQ, Zhou HX, You W (2011) J Am Chem Soc 133:4625
89. Yu G, Gao J, Hummelen JC, Wudl F, Heeger AJ (1995) Science 270:1789
90. Li G, Shrotriya V, Huang J, Yao Y, Moriarty T, Emery K, Yang Y (2005) Nat Mater 4:864

91. Guenes S, Neugebauer H, Sariciftci NS (2007) Chem Rev 107:1324
92. You J, Chen C-C, Hong Z, Yoshimura K, Ohya K, Run X, Shenglin Y, Gao J, Gang L, Yang Y (2013) Adv Mater 25:3973
93. You JB, Dou LT, Yoshimura K, Kato T, Ohya K, Moriarty T, Emery K, Chen CC, Gao J, Li G, Yang Y (2013) Nat Commun 4:1446
94. Tong SW, Wang Yu, Zheng Y, Man-Fai N, Loh KP (2011) Adv Funct Mater 21:4430
95. Tanaka S, Mielczarek K, Ovalle-Robles R, Wang B, Hsu D, Zakhidov AA (2009) Appl Phys Lett 94:113506
96. Mayer AC, Scully SR, Hardin BE, Rowell MW, McGehee MD (2007) Mater Today 10:28
97. Sun Y, Welch GC, Leong WL,Takacs CJ, Bazan GC, Heeger AJ (2011) Nat Mater 11:44
98. Cox PA (1989) The elements: their origin, abundance, and distribution. Oxford University Press, New York
99. Premkumar T, Mezzenga R, Geckeler KE (2012) Small 8:1299
100. Bae S, Kim H, Lee Y, Xu X, Park JS, Zheng Y, Balakrishnan J, Lei T, Ri Kim H, Song YI (210) Nat Nanotechnol 5:574
101. Lee CW, Han X, Chen F, Wei J, Chen Y, Chan-Park MB, Li LJ (2010) Adv Mater 22:1278
102. Lee C, Wei X, Kysar J, Hone W (2008) J Science 321:385
103. Amanda SB, Phys J (2009) Condens Matter 21:144205
104. Gao D, Helander MG, Wang ZB, Puzzo DP, Greiner MT, Lu ZH (2010) Adv Mater 22:5404
105. Zhu H, Wei J, Wang K, Wu D (2009) Sol Energy Mater Sol Cells 93:1461
106. Tung VC, Huang JH, Tevis I, Kim F, Kim J, Chu CW, Stupp SI, Huang J (2011) J Am Chem Soc 133:4940
107. Tung VC, Huang JH, Kim J, Smith AJ, Chu CW, Huang J (2012) Energy Environ Sci 5:7810
108. Bernardi M, Lohrman J, Kumar PV, Kirkeminde A, Ferralis N, Grossman FC, Ren S (2012) ACS Nano 6(10):8896
109. Ramuz MP, Vosgueritchian M, Wei P, Wang C, Gao Y, Wu Y, Chen Y, Bao Z (2012) ACS Nano 6(11):10384